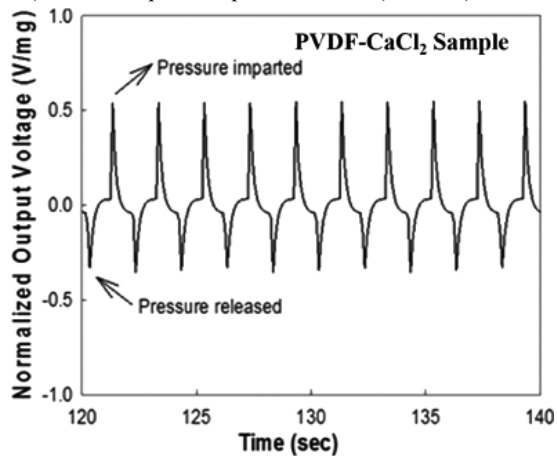

Piezoelectric Characteristics of Electrospun PVDF as a Function of Phase-Separation Temperature and Metal Salt Content

Gajula Prasad, Ponnas Sathiyathan, Arun Anand Prabu*, and Kap Jin Kim*

Macromol. Res., **25**, 00 (2017)

Effect of varying phase-separation temperatures (0 to 70 °C) and chloride salts on the β -crystalline phase of PVDF are investigated in this study. Among the chloride salts, CaCl_2 considerably improved the β -crystalline phase in PVDF. The optimized samples were further electrospun to form nanoweb layers which were used to fabricate the pressure sensors. 70 °C phase-separated PVDF- CaCl_2 sample exhibited higher peak-to-peak piezoelectric output signal (+0.89 V) than neat PVDF (+0.48 V) and 70 °C phase-separated PVDF (+0.53 V).

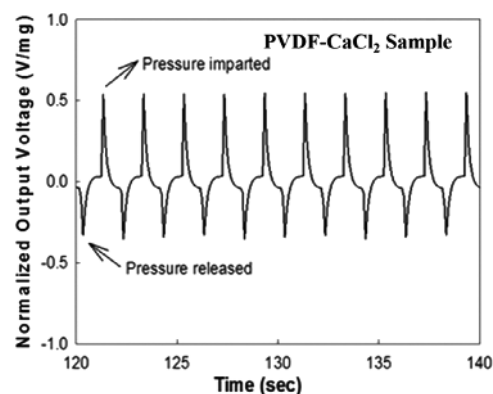


Piezoelectric Characteristics of Electrospun PVDF as a Function of Phase-Separation Temperature and Metal Salt Content

Gajula Prasad¹Ponnan Sathiyathan¹Arun Anand Prabu^{*1}Kap Jin Kim^{*2}¹ Department of Chemistry, School of Advanced Sciences, VIT University, Vellore 632 014, India² Department of Advanced Materials Engineering for Information and Electronics, College of Engineering, Kyung Hee University, Yongin-si, Gyeonggi 17104, Korea

Received December 9, 2016 / Revised May 9, 2017 / Accepted May 31, 2017

Abstract: In this paper, the crystallinity changes in polyvinylidene fluoride (PVDF) as function of varying phase-separation temperatures (0 to 90 °C) and chloride salts (BaCl₂, CaCl₂, CoCl₂, NaCl, SnCl₂, N₂H₆Cl₂) were investigated. FTIR quantitative analysis showed higher β -crystalline and lower α -crystalline content for 70 °C phase-separated PVDF and 70 °C phase-separated PVDF-CaCl₂ (15 wt%) samples. XRD and DSC studies also confirmed the influence of 70 °C phase-separation temperature and CaCl₂ salt in improving the β -crystallinity in PVDF compared to the neat PVDF sample. Since higher β -crystalline content is favoured for use in piezoelectric applications, these two sample preparation conditions were optimized for use in piezoelectric studies. Electrospun nanowebes of the selected samples were measured for their piezoelectric output signals under applied pressure of 1 kgf and released periodically at 0.5 Hz. From the peak-to-peak output voltage, 70 °C phase-separated PVDF-CaCl₂ sample exhibited significantly higher output voltage (+0.89 V) compared to neat PVDF (+0.48 V) and 70 °C phase-separated PVDF (+0.53 V) samples. These results conclude that the combinative effect of phase-separation temperature and metal salt addition plays a vital role in improving the piezoelectric characteristics of PVDF, which signifies the importance of this study.



Keywords: polyvinylidene fluoride, metal salts, electrospinning, crystallinity, piezoelectricity.

1. Introduction

Polyvinylidene fluoride (PVDF), a semi-crystalline polymer with $-(CF_2-CH_2)-$ repeating units is one of the most widely used materials for diverse applications such as piezoelectric sensors,¹⁻⁴ data storage devices,⁵⁻⁸ membranes,⁹⁻¹³ super-hydrophobic coatings,¹⁴⁻¹⁶ etc. Though PVDF exhibit at least four different crystalline (α , β , γ , and δ) forms, the β -crystalline form is mainly responsible for its high performance characteristics. β -crystals in PVDF can be enhanced by converting either amorphous or α -crystalline phases into β -crystalline phase.¹⁷⁻¹⁹ Most widely employed routes to enhance β -crystallinity in PVDF include fabrication of samples using spin-casting or electrospinning methods instead of the conventional solution-casting method,^{1,4,17,19} using mixed solvents (DMF-acetone, 60/40 ratio) instead of single solvent (DMF only)^{4,17,19} and thermal treatment under vacuum (130 °C, 3 h).^{4,19} Other methods employed include conversion of α -crystals in PVDF into β -crystals using

uni- or bi-directional drawing of PVDF films,²⁰ poling under high electric field,²¹ or by crystallization from melt.²²

Many researchers have also used metal nanoparticles and metal salts as fillers in PVDF and studied their effect in improving the β -crystallinity of PVDF.^{5,23-34} Crystalline phase changes in the modified polymer depends on the chemical nature of the metal filler and the ways in which the metal interact with the host matrix. In the case of metals salts, one of our earlier report has investigated the effect of varying mass fractions (0 to 20 wt%) of calcium chloride (CaCl₂) metal salt on the α - and β -phase content of PVDF as-cast films.⁵ Maximum β -phase was achieved for PVDF-CaCl₂ (15 wt%) compared to neat PVDF sample. The applicability of modified PVDF thick film as a ferroelectric insulator was also demonstrated in a one-capacitor type random access memory device with a remnant polarization of 3.1 $\mu\text{C}/\text{cm}^2$. This served as evidence that the un-oriented PVDF-CaCl₂ as-cast film can be used in electronic applications without any further stretching process. In a recent study, Jana *et al.* used a hydrated metal salt (MgCl₂·6H₂O) as filler in PVDF to fabricate high performance piezoelectric energy harvesters delivering an open circuit voltage of 4 V under a pressure of around 4.45 kPa.³⁵ The generated power was also sufficient to turn on at least ten commercial blue LEDs. The enhanced piezo-response is attributed to the combined effect of the change in the inherent dipole moment of the electroactive phase containing PVDF itself and H-bonding arising

Acknowledgments: This work was supported by the Industrial Strategic Technology Development Program (Grant No. 10047976) funded by the Ministry of Trade, Industry & Energy (MOTIE, KOREA). The authors would also like to thank Dr. R. P. S. Chakradhar and Dr. Parthasarathi Bera, CSIR-NAL, Bangalore, India and Mr. T. Sai Kiran, VIT University, India for helping in the characterization studies.

***Corresponding Authors:** Arun Anand Prabu (anandprabu@vit.ac.in), Kap Jin Kim (kjkim@khu.ac.kr)

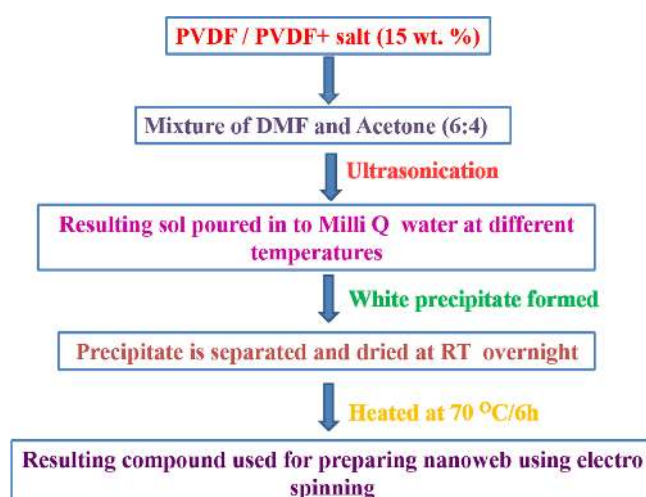
between the Mg-salt filler and PVDF *via* electrostatic interactions.

Few research groups have also studied the effect of phase-separation temperatures on the crystalline phase changes in PVDF. In one such instance, Ma *et al.* prepared PVDF microporous membranes *via* thermally induced phase-separation method by quenching the PVDF samples at 100, 110, and 118 °C.³⁶ In another recent study, Chakradhar *et al.* studied the structural changes in PVDF based super-hydrophobic coatings as a function of varying phase-separation temperatures (100 to 350 °C). A transformation of the PVDF coating from super-hydrophobic at 300 °C (water contact angle: 150°) to super-hydrophilic at 350 °C phase-separation temperature (water-contact angle: 10°) was reported, and the unusual wetting characteristics are attributed to both the chemical composition and geometric microstructure of the PVDF surface.³⁷

Though the above literature survey dealt with the effect of metal salts and phase-separation temperature on the crystalline phase changes in PVDF as-cast films, as per our knowledge, no previous studies have reported their effect on PVDF electrospun nanofibers, and more specifically on the piezoelectric characteristics of PVDF electrospun nanofiber web samples. Hence, the present study is devoted to investigating the effect of varying phase-separation temperatures (0 to 90 °C) and metal chloride salt content (15 wt% of PVDF) on the crystalline phase changes in PVDF. Based on the optimized conditions of phase-separation temperature and metal salt type, the modified PVDF is electrospun to form nanofiber mat which is used as an active material in a pressure sensor and studied for its piezoelectric characteristics. The results are discussed in detail.

2. Experimental

PVDF (Pragathi Chemicals, India), DMF, acetone, ethanol (Loba Chemie, India), and different chloride salts (BaCl₂, CaCl₂, CoCl₂, NaCl, SnCl₂, N₂H₆Cl₂, from Merck, India) were used as received. Sample preparation involved two different pathways. In the first instance, as-cast samples of PVDF were prepared as a function of phase-separation temperatures and metal chloride salts as follows: a known amount of neat PVDF is dispersed in DMF:acetone solvent mixture (60:40 (v/v)) using ultrasonication until an homogeneous clear solution is obtained. The clear solution of PVDF is poured into 80 mL of Milli-Q water maintained at varying temperatures (0, 30, 50, 70, and 90 °C) under continuous stirring. The resultant white-coloured precipitate is separated using Whatman filter paper and washed twice with water and once with ethanol. The final product is dried in a hot-air oven at 70 °C for 6 h and then stored in a desiccator for further use. PVDF is also mixed with different chloride salts (15 wt% of PVDF content) at 70 °C phase-separation temperature and the final products were stored in a desiccator for further use. Since our final objective is to fabricate a piezoelectric sensor based on electrospun PVDF nanofiber mat, the second pathway is limited to electrospinning of the optimized samples, *viz.* neat PVDF, 70 °C phase-separated PVDF and 70 °C phase-separated PVDF-CaCl₂ samples prepared from the first step.



Scheme 1. Schematic procedure for the preparation of phase-separated PVDF.

The complete preparation pathways are shown in Scheme 1.

FTIR studies were performed by Shimadzu IR Affinity-1 spectrometer using KBr pellet at a resolution of 4 cm⁻¹ with 100 scans. Phase purity of as-prepared solid samples was measured using BRUKER D8 Advance X-ray diffractometer. Monochromatic Cu K α radiation ($\lambda=0.1548$ nm) was used and the samples were scanned from 15° to 30° at a scanning rate of 0.02°/min. Surface morphology of the samples was examined by scanning electron microscopy (LEO 440i, UK). Non-isothermal curves of the samples were measured using DSC (Perkin Elmer). 5 mg of as-prepared solid samples were taken and heated from 100 °C to 200 °C with a heating rate of 10 °C/min under oxygen atmosphere. X-ray photoelectron spectroscopy (XPS) of the samples was recorded using a SPECS spectrometer using 150 W non-monochromatic AlK α radiation (1486.6 eV) as an X-ray source. The binding energies reported here were taken as reference with C1s peak at 284.6 eV. Individual spectra were recorded with 40 eV pass energy with 0.05 eV step increment.

Electrospinning was carried out using eSprayTM setup (NanoNC, Korea) at ambient temperature under the following conditions: solution concentration 18 wt% (w/v), solvent used is DMF: Acetone mixture (60:40 (v/v)), solution volume 6 mL, flow rate 1.5 cc/h, tip-to-collector distance 10 cm, needle size 18G, applied DC voltage 12 kV and collector rotating speed 80 rpm. Piezoelectric sensors were fabricated by attaching a nickel-copper plated conductive fabric of 2 cm diameter (J. G. Korea Inc., Korea) to each side of the nanofiber web as top and bottom electrodes, and further encapsulated using adhesive transparent tape for protection. The fabricated pressure sensors were used for measuring their piezoelectric output signal (V/mg) under a load of 1 kgf imparted to the nanofiber web sensor using a hammer of 2 cm diameter and released periodically at 0.5 Hz. The output peak-to-peak voltage (V_{p-p}) was measured using a custom-made dynamic pressure instrument and the signals were transferred to the preamplifier (Piezo Film Lab Amplifier, Measurement Specialties Inc., USA).

3. Results and discussion

Numerous reports are available in the literature utilizing FTIR to study the different crystalline structures of PVDF. In general, PVDF exhibit characteristic α -crystalline phase absorption bands at 486, 532, 613, 763, 796, and 976 cm^{-1} , β -crystalline bands at 509, 840, and 1279 cm^{-1} and γ -crystalline phase bands at 1232 cm^{-1} .^{5,17,18} In our study, the 70 °C phase-separated PVDF sample exhibited higher β -crystalline phase when compared to other phase-separated temperatures as well as neat PVDF as shown qualitatively and quantitatively in Figures 1(a) and 2(a), respectively. With increasing phase-separation temperature, the β -crystalline phase in PVDF increases gradually along with corresponding decrease in α -crystalline phase up to 70 °C. How-

ever, the β -crystalline phase in 90 °C phase-separated PVDF drops back to the neat PVDF level, which may be attributed to the reduction in crystallization rate with increasing temperature from 70 to 90 °C. At temperatures up to 70 °C, PVDF chains have lesser mobility and have sufficient time to convert thermal energy to thermodynamically meta-stable β -crystalline phase.³⁸ On the other hand, the 90 °C phase-separation temperature is nearer the evaporation temperature of water and as the water level gets lower in the phase-separation chamber with time, it exhibits a crystalline behaviour similar to that of neat PVDF (in the dry state).

Similarly, for the crystalline studies carried out as a function of different chloride salts, CaCl_2 containing PVDF exhibited higher β -crystalline and lower α -crystalline phases as shown

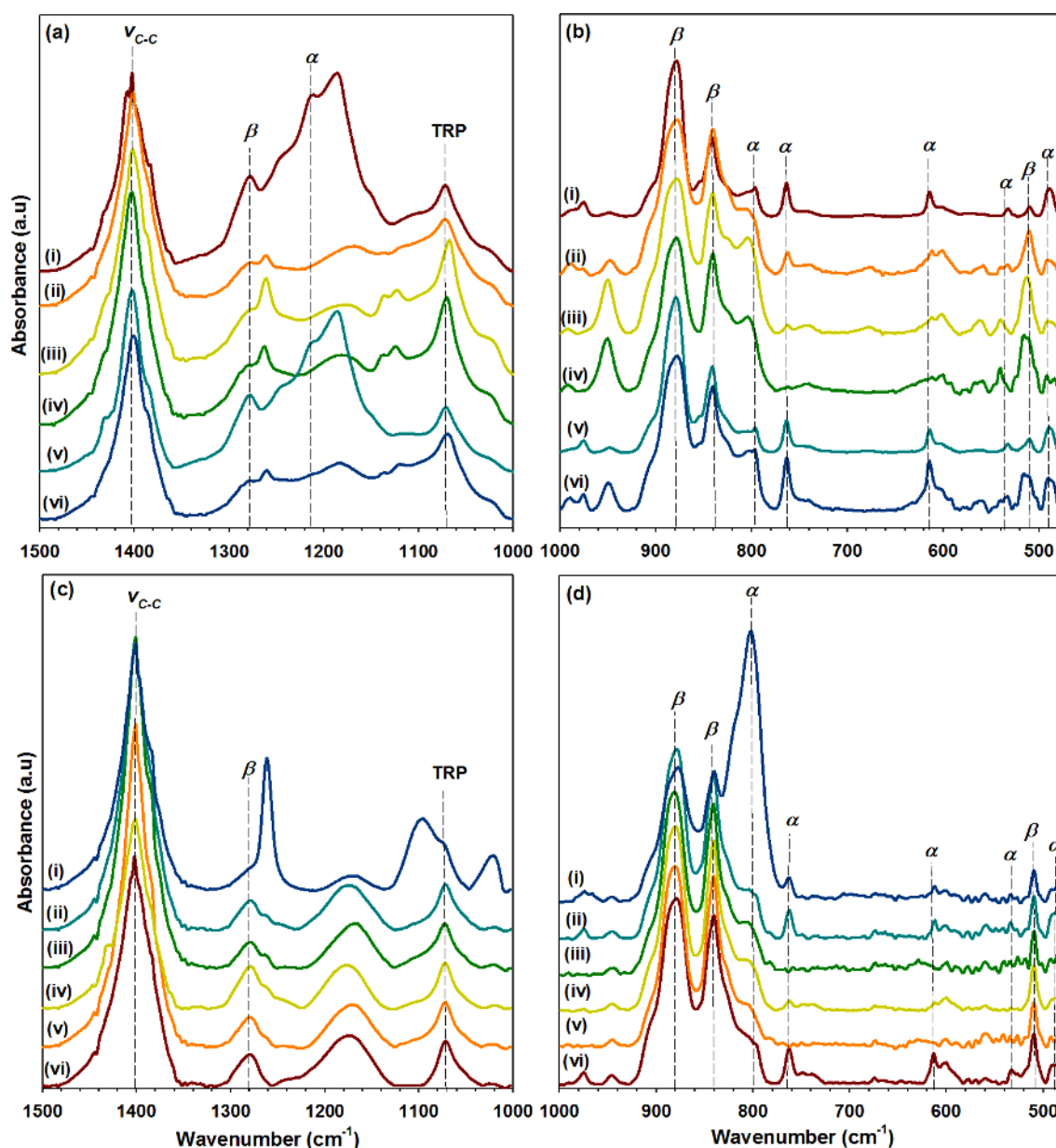


Figure 1. FTIR qualitative analysis: Crystalline phase changes in (i) neat PVDF under varying phase-separation temperatures: (ii) 0 °C, (iii) 30 °C, (iv) 50 °C, (v) 70 °C, and (vi) 90 °C exhibited in the regions 1500-1000 cm^{-1} (a) and 1000-475 cm^{-1} (b), respectively. Crystalline phase changes in 70 °C phase-separated PVDF containing different metal chloride salts: (i) SnCl_2 , (ii) NaCl , (iii) $\text{N}_2\text{H}_6\text{Cl}_2$, (iv) CoCl_2 , (v) CaCl_2 , and (vi) BaCl_2 exhibited in the regions 1500-1000 cm^{-1} (c) and 1000-475 cm^{-1} (d), respectively.

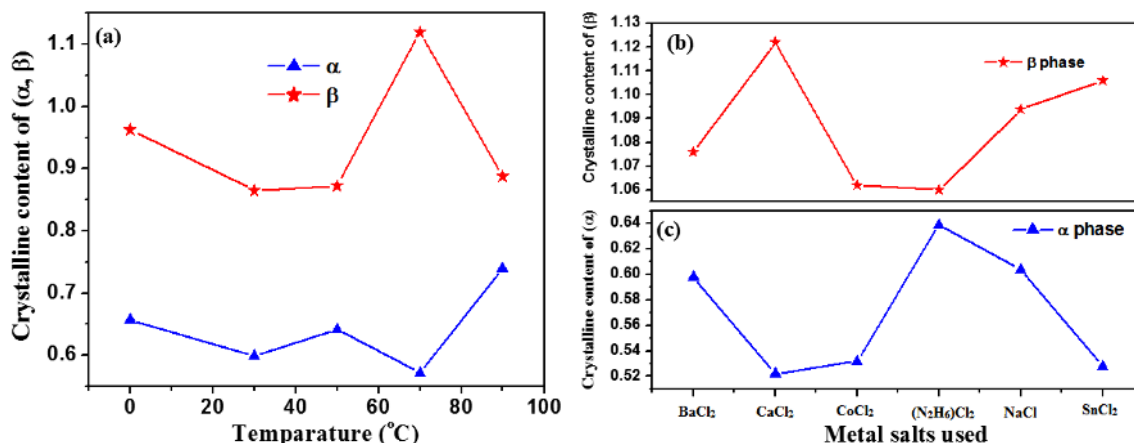


Figure 2. FTIR quantitative analysis: Estimation of crystalline content (α and β) in neat PVDF under varying phase-separation temperatures (a), and in 70 °C phase-separated PVDF containing different metal chloride salts (b), (c).

qualitatively and quantitatively in Figures 1(b) and 2(b), (c), respectively. In our earlier report too, FTIR technique was used to confirm the higher β -crystallinity in PVDF induced by the addition of CaCl₂ salt over other chloride salts such as NaCl, KCl, FeCl₃, NiCl₂, CuCl₂ and MgCl₂.⁵ In the present study, FTIR quantitative analysis (Figure 2) of α - (613 cm⁻¹), β - (1279 cm⁻¹), and γ -crystalline phases (1232 cm⁻¹) were carried out with respect to thickness relative peak (at 1072 cm⁻¹) in order to compensate for the changes in film thickness due to different sample preparation conditions.^{19,39} Relative increase in β -crystallinity along with decreasing α -crystallinity with increasing phase-separation temperature from 30 °C to 70 °C was observed but which shows a decreasing trend at higher temperatures. Among all the phase-separation temperatures used in this study, 70 °C sample exhibited highest β -crystalline phase. Likewise, among different chloride salts used in this study, CaCl₂ contained PVDF sample exhibited higher β - and lower α -crystalline content.

Figure 3 shows the XRD patterns of phase-separated PVDF and PVDF-CaCl₂ samples. Compared to neat PVDF, the peaks at $2\theta=18.2$, 20.04, and 26.5° corresponding to α -phase shows a decreasing trend with increasing phase-separation temperature up to 70 °C. The peak at 20.04° corresponding to α -crystal-

line phase is shifted towards higher region (20.30°) which is assigned to the β -crystalline phase. In contrast, the 90 °C phase-separated PVDF sample exhibited similar patterns to that of neat PVDF, which confirms the earlier FTIR data of increasing β -crystalline phase up to 70 °C and decreasing β -crystallinity at higher phase-separation temperatures. The α -crystalline phase of neat PVDF at 20.04° is further shifted to higher region at 20.4° upon the addition of CaCl₂ (Figure 3(b)), which serves as an evidence of the vital role played by CaCl₂ salt in increasing the β -crystalline phase of PVDF.

Figure 4 shows the SEM micrographs of neat PVDF (a), (b), 30 °C phase-separated PVDF (c), (d), 70 °C phase-separated PVDF (e), (f) and 70 °C phase-separated PVDF-CaCl₂ (g), (h) at two different magnifications, 500× and 1500×, respectively. Compared to neat PVDF (Figure 4(a), (b)), the phase-separated samples (Figure 4(c)-(h)) were found to exhibit thread-like morphology with tiny continuous pores. The surface morphology of phase-separated PVDF samples also changed remarkably with temperature as observed from increasing thread diameter with increasing temperature (from 30 to 70 °C) along with proportionate decrease in porosity (Figure 4(c)-(f)). In the case of PVDF-CaCl₂ sample, it looked like CaCl₂ salt particles

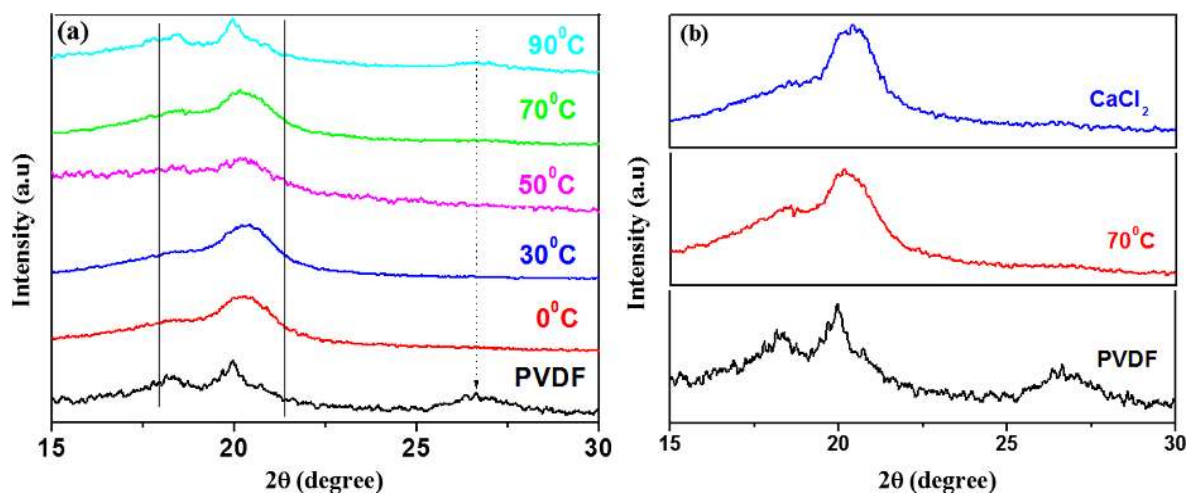


Figure 3. XRD analysis: Estimation of crystalline content in neat PVDF under varying phase-separation temperatures (a), and in 70 °C phase-separated PVDF-CaCl₂ (b).

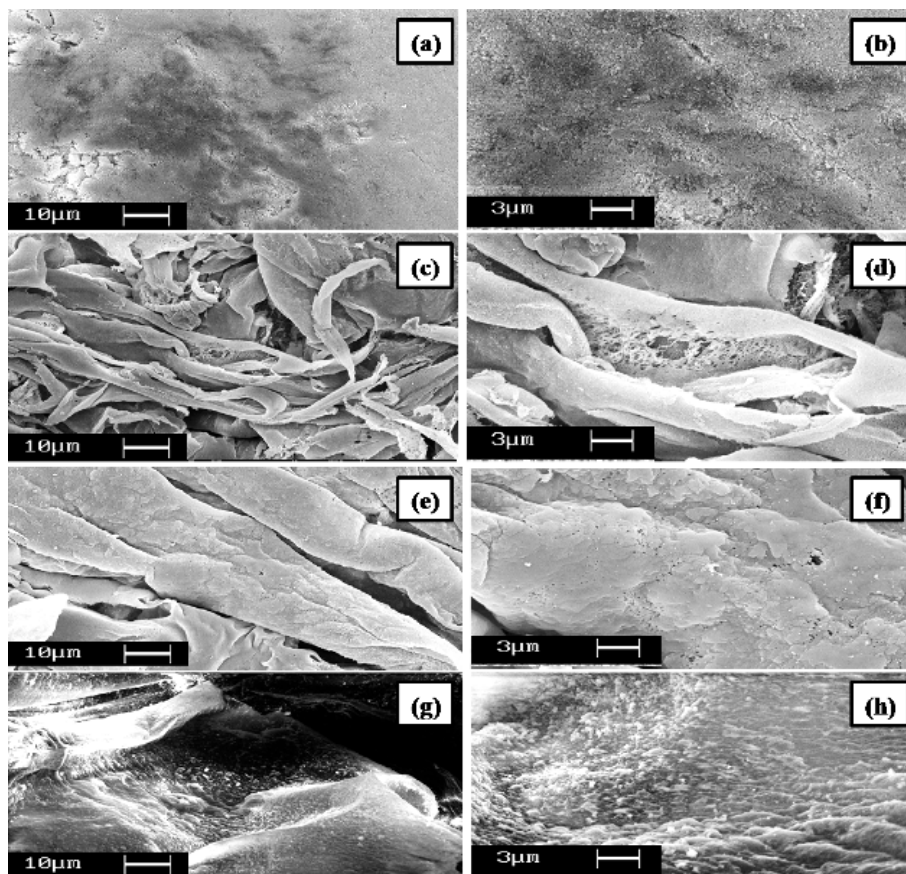


Figure 4. SEM images for neat PVDF (a), (b), 30 °C phase-separated PVDF (c), (d), 70 °C phase-separated PVDF (e), (f), and 70 °C phase-separated PVDF-CaCl₂ (g), (h) at two different magnifications, 500× and 1500×, respectively.

Table 1. Elemental analysis for neat PVDF and phase-separated PVDF samples

Samples used	Elemental %			
	C	F	Ca	Cl
Neat PVDF	64.73	35.27	-	-
30 °C phase-separated PVDF	68.10	31.90	-	-
70 °C phase-separated PVDF	65.55	34.45	-	-
70 °C phase-separated PVDF-CaCl ₂	51.59	46.30	0.85	1.26

were seated on the polymer matrix, though the SEM data cannot provide any evidence towards the changes in crystalline nature of the studied samples.

Table 1 shows the elemental analysis carried out using energy dispersive spectroscopy (EDS). Except PVDF-CaCl₂ sample, all the other samples showed almost similar composition which denotes that there is no loss in the starting material even after phase-separation. On the other hand, PVDF-CaCl₂ sample showed decreasing elemental (%) of C and proportionate increase in elemental (%) of F along with negligible amount (2%) of CaCl₂ salt. Even though the added CaCl₂ content is 15 wt% to that of the PVDF content at the beginning of time, after several washings with water, the loosely bonded CaCl₂ salt was removed from the matrix resulting in lesser remaining CaCl₂ salt from EDS analysis.

From Figure 5(a), it is clear that the neat PVDF exhibits doublet endothermic peak (159.6 and 163.6 °C) with a pin differ-

ence of 4 °C. In general, neat PVDF sample consists of two different crystalline phases,⁴⁰ namely lower temperature peak assigned to α -phase and higher temperature peak assigned to β -phase.^{37,41,42} Compared to neat PVDF, the phase-separated samples (except the 90 °C) exhibited an unique trend with the disappearance of peak at lower temperature region (159.6 °C), whereas the higher temperature peak at 163.6 °C in neat PVDF is almost same as in 30 °C phase-separated sample and slightly moved to higher temperature (164.3 °C) in 70 °C phase-separated sample. Interestingly, the 90 °C phase-separated sample exhibited a doublet peak at 160.2 and 163.6 °C assigned to β - and α -crystalline phases, respectively (highlighted in enlarged image in Figure 5(a)). The 70 °C phase-separated PVDF-CaCl₂ also exhibited a unique peak at 160.9 °C assigned as β -crystalline phase which is moved towards lower temperature from 163.6 °C as shown in Figure 5(b). This might have appeared due to the presence of Ca²⁺ ions in the matrix which acts as nucleation sites.²² From these results, we can conclude that the phase-separated PVDF samples (except at 90 °C) exhibit a distinct β -crystalline phase, whereas neat PVDF and 90 °C phase-separated PVDF samples exhibit a mixture of α and β -crystalline phases.

XPS of C1s core levels in neat PVDF and phase-separated PVDF with different conditions are shown in Figure 6. Two dominant peaks appearing at 285.6 and 290.5 eV correspond to -CH₂- and -CF₂-, respectively. CF₂/CH₂ ratios of neat PVDF, phase-separated PVDF (30 and 70 °C) and 70 °C phase-sepa-

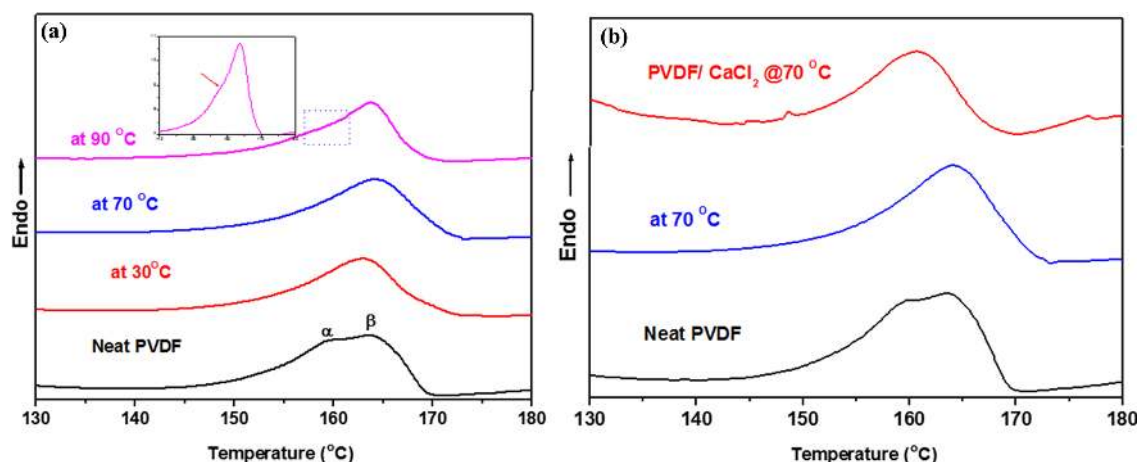


Figure 5. DSC curves of neat PVDF under varying phase-separation temperatures (inset showing a very small peak at 160.2 °C attributed to α -crystalline phase) (a), and of 70 °C phase-separated PVDF- CaCl_2 (b).

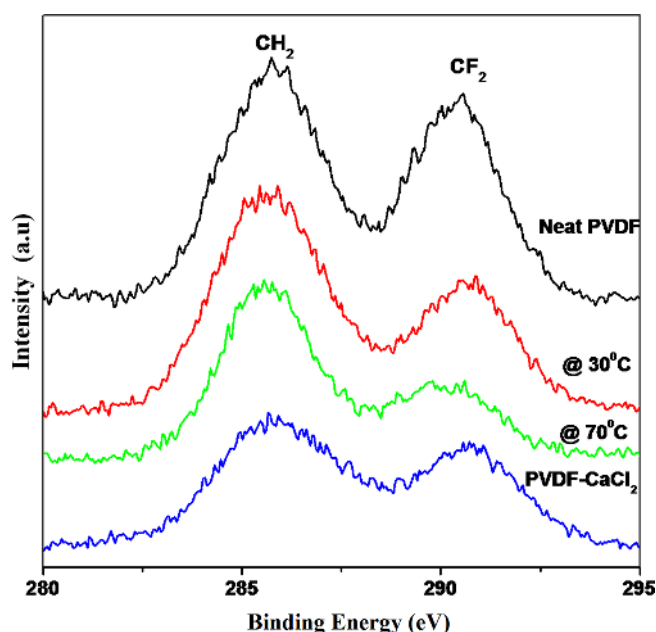


Figure 6. XPS of C1s core levels in neat PVDF, phase-separated PVDF (at 30 and 70 °C) and 70 °C phase-separated PVDF- CaCl_2 .

rated PVDF- CaCl_2 is calculated to be 0.77, 0.41, 0.55, and 0.85, respectively. XPS results demonstrate decreasing fluorine amount in the case of 30 and 70 °C phase-separated samples, whereas the PVDF- CaCl_2 sample exhibited enhanced fluorine content. A similar trend in fluorine content is also observed from EDS analysis. This difference in fluorine content may have arisen from the changes in the chain orientation of polymer which in turn is dependent on the sample preparation conditions and effect of CaCl_2 - CF_2 interactions. Further studies were carried out using the optimized samples, viz. neat PVDF, 70 °C phase-separated PVDF and 70 °C phase-separated PVDF- CaCl_2 (15 wt%).

Figure 7 shows the simple equivalent circuit diagram and setup used for measuring the piezoelectric signal under dynamic pressure.⁴³ Figure 8 shows the normalized piezoelectric output voltage (V/mg) generated from the piezoelectric sensor with a change in the total polarization as a function of time

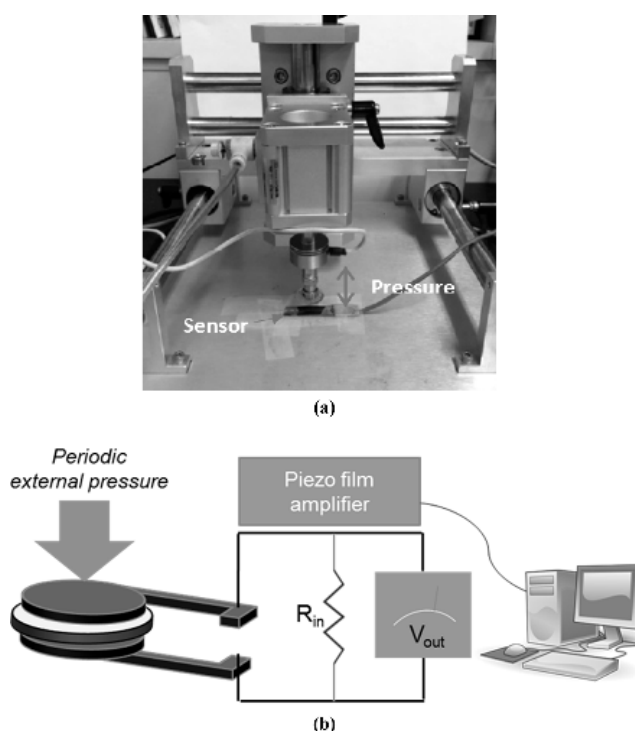


Figure 7. Setup for measuring dynamic pressure (a) and equivalent circuit diagram for measuring piezoelectric signal (b).

during the imparting and releasing of external pressure. This data serves as evidence that the materials used in this study can be effectively used as a ‘nanogenerator’ to generate energy with higher efficiency. From the piezoelectric output signal measured for neat PVDF, 70 °C phase-separated PVDF and 70 °C phase-separated PVDF- CaCl_2 samples, the chloride salt containing PVDF showed higher increase in the peak-to-peak output voltage. This is an evidence for the significant contribution of CaCl_2 salt towards enhancing the piezoelectric output voltage of PVDF sensor. Compared to the neat PVDF (+0.48 V), the phase-separated PVDF exhibited a moderate increase in the output voltage (+0.53 V), which further improved significantly to +0.89 V for PVDF- CaCl_2 sample. In the case of piezoelectric sensors fabricated using electrospun PVDF nanoweb

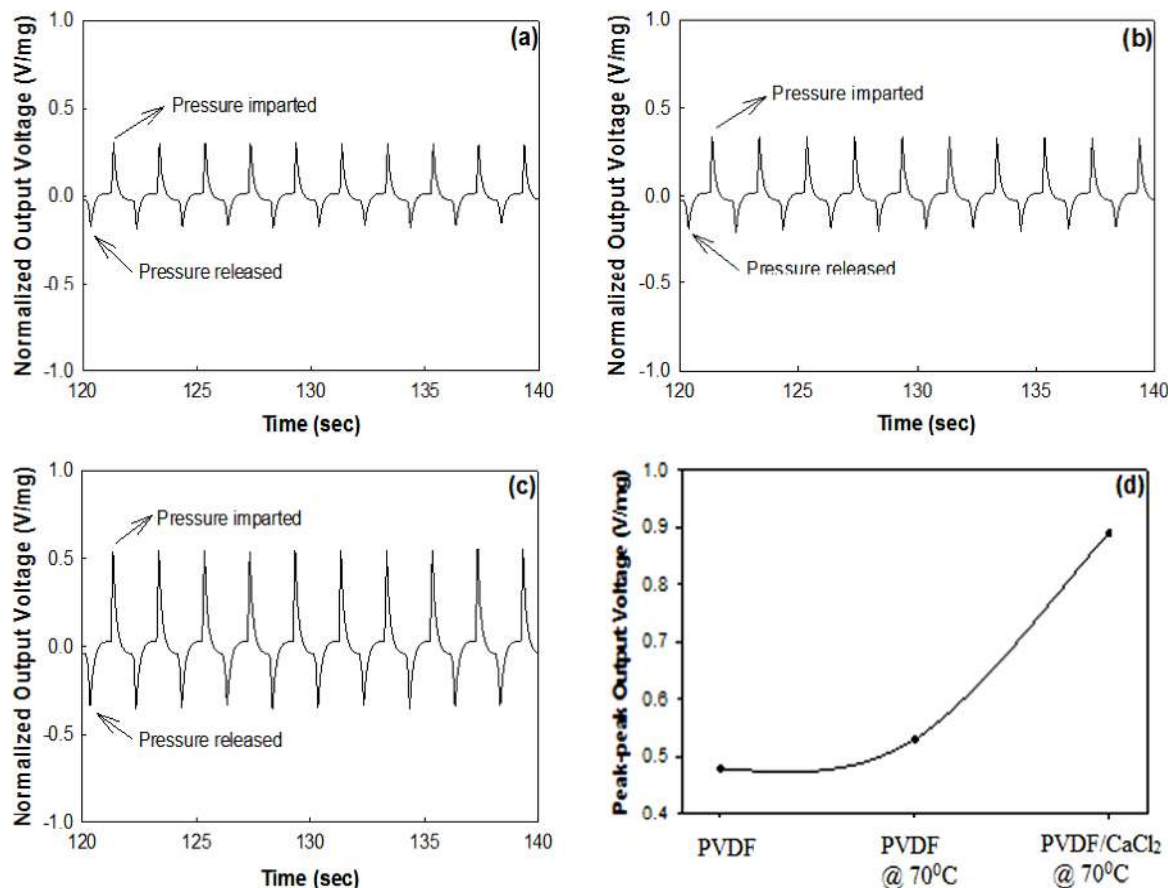


Figure 8. Normalized piezoelectric output voltage (V/mg) measured for electrospun samples: neat PVDF (a), 70 °C phase-separated PVDF (b), and 70 °C phase-separated PVDF-CaCl₂ (c). Peak-to-peak output voltage (V/mg) measured for the above samples (d).

fibers, the piezoelectric characteristics are attributed to the existence of higher β -crystalline phase content arising from favorable orientation of the C-F and C-H dipoles in PVDF along the poling direction (perpendicular to C-C direction).² Addition of CaCl₂ salt in PVDF further induced higher β -phase content along with reduced α -crystalline phase, which serves as an evidence of the crystalline phase-transformation from α - to β -crystalline phase in the case of PVDF-CaCl₂ sample. From the electrical measurements, we propose a mechanism of interaction between Ca²⁺, DMF solvent and C-F dipoles in PVDF as follows: Ca²⁺...O=C=N⁺...F⁻-C⁺. Molecular interactions between PVDF and DMF along with the additional presence of CaCl₂ tend to orient the packing of CH₂-CF₂ dipoles locally resulting in all-*trans* conformation and thereby higher β -crystalline phase in PVDF-CaCl₂ sample. Comparing between Figure 8(a) and Figure 8(b), even though the phase-separation temperature (70 °C) has an effect in improving the β -crystalline content in PVDF, a significant relaxation in chain-dipole orientation may have occurred inherently, thereby resulting in lower all-*trans* conformation compared to the PVDF-CaCl₂ sample as shown in Figure 8(c), and quantitatively shown in Figure 8(d). Overall, the studies carried out in this work serves as evidence for the vital role played by the phase separation temperature and chloride salt in influencing the crystalline phases in PVDF.

4. Conclusions

A facile method to increase the β -crystalline phase of PVDF was investigated as a function of varying phase-separation temperatures and chloride salts. FTIR and XRD spectral analysis of neat PVDF demonstrate increasing β -crystallinity along with corresponding decrease in α -crystallinity with increasing phase-separation temperature from 0 to 70 °C, and this trend is reversed at higher phase-separation temperatures. Among the chloride salts, the addition of CaCl₂ improved the β -crystalline phase in PVDF. DSC results of neat PVDF revealed a doublet endothermic peak at 159.6 °C and 163.6 °C corresponding to α - and β -crystalline phases, respectively. On the other hand, the phase-separated PVDF and PVDF-CaCl₂ samples exhibited a single endothermic peak at 164.3 °C assigned to β -crystalline phase. XPS results also revealed higher β -crystalline phase in PVDF-CaCl₂ sample aided by increasing fluorine content due to proper alignment of C-H and C-F dipoles. The optimized samples, *viz.* neat PVDF, 70 °C phase-separated PVDF and 70 °C phase-separated PVDF-CaCl₂ were used for piezoelectric measurements. Their electrospun nanoweb samples were used to fabricate pressure sensors and among the three samples, 70 °C phase-separated PVDF-CaCl₂ sample exhibited higher peak-to-peak piezoelectric output signal (+0.89 V) than neat PVDF (+0.48 V) and 70 °C phase-separated PVDF (+0.53 V). Overall,

the present study is very much useful in understanding the crystalline phase changes in PVDF samples prepared under different conditions (thermal phase-separation and electrospun nanoweb), and serves as an evidence that the PVDF-CaCl₂ nanofiber web can be used as an active material in flexible pressure sensor and energy-harvesting applications.

References

- (1) S. Yoon, A. A. Prabu, S. Ramasundaram, and K. J. Kim, *Adv. Sci. Technol.*, **60**, 52 (2008).
- (2) S. Lee, Y. J. Ahn, A. A. Prabu, and K. J. Kim, *J. Fiber Bioeng. Inform.*, **6**, 369 (2013).
- (3) Y. Mao, P. Zhao, G. McConohy, H. Yang, Y. Tong, and X. Wang, *Adv. Energy Mater.*, **4**, 1301624 (2014).
- (4) P. Sathiyathan, A. A. Prabu, and K. J. Kim, *Macromol. Res.*, **24**, 670 (2016).
- (5) S. Yoon, A. A. Prabu, K. J. Kim, and C. Park, *Macromol. Rapid Commun.*, **29**, 1316 (2008).
- (6) Y. J. Park, S. J. Kang, B. Lotz, M. Brinkmann, A. Thierry, K. J. Kim, and C. Park, *Macromolecules*, **41**, 8648 (2008).
- (7) S. J. Kang, Y. J. Park, I. Bae, K. J. Kim, H.-C. Kim, S. Bauer, E. L. Thomas, and C. Park, *Adv. Funct. Mater.*, **19**, 2812 (2009).
- (8) Y. J. Park, I. Bae, S. J. Kang, J. Chang, and C. Park, *IEEE Trans. Dielectr. Electr. Insul.*, **17**, 1135 (2010).
- (9) W. Zhang, Z. Shi, F. Zhang, X. Liu, J. Jin, and L. Jiang, *Adv. Mater.*, **25**, 2071 (2013).
- (10) S. A. Pervin, A. A. Prabu, K. J. Kim, and Y. T. Lee, *Macromol. Res.*, **23**, 86 (2015).
- (11) W. Jang, J. Yun, K. Jeon, and H. Byun, *RSC Adv.*, **5**, 46711 (2015).
- (12) C. Liu, X. Li, T. Liu, Z. Liu, N. Li, Y. Zhang, C. Xiao, and X. Feng, *J. Membr. Sci.*, **512**, 1 (2016).
- (13) W. Zhang, Y. Zhang, R. Fan, and R. Lewis, *J. Nanopart. Res.*, **18**, 31 (2016).
- (14) R. P. S. Chakradhar, G. Prasad, P. Bera, and C. Anandan, *Appl. Surf. Sci.*, **301**, 208 (2014).
- (15) G. Prasad and A. A. Prabu, *Adv. Mater. Res.*, **938**, 199 (2014).
- (16) G. Prasad and A. A. Prabu, *Res. J. Pharm. Biol. Chem. Sci.*, **7**, 1808 (2016).
- (17) D. M. Dhevi, A. A. Prabu, M. Pathak, and K. J. Kim, *Adv. Mater. Res.*, **584**, 197 (2012).
- (18) D. M. Dhevi, A. A. Prabu, and M. Pathak, *Polymer*, **55**, 886 (2014).
- (19) D. M. Dhevi, A. A. Prabu, and K. J. Kim, *J. Mater. Sci.*, **51**, 3619 (2016).
- (20) L. David, J. L. Winsor, and B. A. Scheinbeim, *J. Polym. Sci., Part B*, **34**, 2967 (1996).
- (21) J. Scheinbeim, C. Nakafuku, B. A. Newman, and K. D. Pae, *J. Appl. Phys.*, **50**, 4399 (1979).
- (22) A. J. Lovinger, *Polymer*, **22**, 412 (1981).
- (23) H. Szalińska and M. Pietrzak, *Polym. Plast. Technol. Eng.*, **19**, 107 (1982).
- (24) T. R. Hebner, C. C. Wu, D. Marcy, M. H. Lu, and J. C. Sturm, *Appl. Phys. Lett.*, **72**, 519 (1998).
- (25) J. Park, Y. Seo, I. Kim, C. Ha, K. Aimi, and S. Ando, *Macromolecules*, **37**, 429 (2004).
- (26) S. M. Lebedev, O. S. Gefle, and S. N. Tkachenko, *J. Electrostat.*, **68**, 122 (2010).
- (27) S. M. Lebedev, O. S. Gefle, and M. V. Semenikhin, *J. Korean Powder Metall. Inst.*, **18**, 181 (2011).
- (28) R. H. Upadhyay and R. R. Deshmukh, *J. Electrostat.*, **71**, 945 (2013).
- (29) J. G. Lee, S. H. Kim, H. C. Kang, and S. H. Park, *Macromol. Res.*, **21**, 349 (2013).
- (30) J. Yu, W. Wu, D. Dai, Y. Song, C. Li, and N. Jiang, *Macromol. Res.*, **22**, 19 (2014).
- (31) P. Thakur, A. Kool, B. Bagchi, S. Das, and P. Nandy, *Appl. Clay Sci.*, **99**, 149 (2014).
- (32) J. H. Lee, S. J. Kim, J. S. Park, and J. H. Kim, *Macromol. Res.*, **24**, 909 (2016).
- (33) S. G. Lee, J. W. Ha, E. H. Sohn, I. J. Park, and S. B. Lee, *Appl. Surf. Sci.*, **390**, 339 (2016).
- (34) S. Biswas and S. Bhattacharya, *Thermochim. Acta*, **649**, 69 (2017).
- (35) S. Jana, S. Garain, S. Sen, and D. Mandal, *Phys. Chem. Chem. Phys.*, **17**, 17429 (2015).
- (36) W. Ma, S. Chen, J. Zhang, and X. Wang, *J. Macromol. Sci. Part B: Phys.*, **50**, 1 (2011).
- (37) R. P. S. Chakradhar, G. Prasad, P. Bera, and C. Anandan, *Appl. Surf. Sci.*, **301**, 208 (2014).
- (38) J. Liu, X. Lu, and C. Wu, *Membranes*, **3**, 389 (2013).
- (39) K. J. Kim, Y. J. Cho, and Y. H. Kim, *Vib. Spectrosc.*, **9**, 147 (1995).
- (40) B. E. E. Mohajir and N. Heymans, *Polymer*, **42**, 5661 (2001).
- (41) P. Sajkiewicz, *Eur. Polym. J.*, **35**, 1581 (1999).
- (42) R. Gregorio and R. C. Capita, *J. Mater. Sci.*, **35**, 299 (2000).
- (43) S. J. Lee, A. A. Prabu, and K. J. Kim, *Mater. Lett.*, **148**, 58 (2015).